Parity Breaking and Solitary Waves in Axisymmetric Taylor Vortex Flow

Richard J. Wiener[(a)] and Daniel F. McAlister[(b)]

Department of Physics, Lewis and Clark College, Portland, Oregon 97219

(Received 6 August 1992)

We report, for the first time, the experimental observation of solitary waves in an axisymmetric Taylor-Couette flow. The solitary waves result from a parity-breaking bifurcation which occurs near the onset of Eckhaus instability for Taylor vortex flow in a wide-gap, counterrotating system (radius ratio $\eta = 0.5$ and speed ratio $\mu = -0.2$). Our results agree quantitatively with a recent theoretical calculation by Riecke and Paap.

PACS numbers: 47.20.Ky, 47.20.Ft, 47.35.+i

Parity-breaking bifurcations, which lead to propagative spatiotemporal dynamics, have been found recently in several nonlinear pattern-forming systems that involve interfacial instabilities. For instance, a parity-breaking bifurcation occurs in directional solidification of liquid crystal [1] and in the viscous fingering of a liquid film between moving surfaces [2]. In both of these systems, the parity-breaking bifurcation leads to solitary waves which travel through an otherwise spatially periodic and stationary interface. Theoretical calculations indicate that the parity-breaking bifurcations arise due to resonant interaction of spatial modes (with wave numbers q and $2q$) [3-7]. Riecke and Paap (RP) have conjectured that resonant interaction of spatial modes should generate a parity-breaking bifurcation leading to rich dynamics in a wide range of pattern-forming systems, if their symmetries allow mode interaction, not just in interfacial systems [8].

RP investigated this conjecture theoretically by studying Taylor-Couette flow, the flow of fluid between concentric rotating cylinders [9]. They chose this classical pattern-forming system since it is known that the q-$2q$ resonant mode interaction plays an active role in the dynamics of the system by deforming the Eckhaus stable band of wave numbers for stationary Taylor vortices, if the gap between the cylinders is wide [10-12]. Moreover, starting from the basic equations of motion, linear stability analysis of Taylor-Couette flow allows detailed quantitative calculations of bifurcation boundaries. Such calculations do not yet exist for the directional solidification or viscous fingering systems. RP performed a linear stability analysis on axisymmetric Taylor vortex flow (TVF) and found that a parity-breaking bifurcation, which results from the q-$2q$ resonant mode interaction and is not preempted by the Eckhaus instability, does indeed occur for flow between counterrotating cylinders in a wide-gap system [8]. RP also modeled the nonlinear evolution of the parity-breaking mode and found that their model allows for a localized inclusion of drift waves, similar to the solitary waves previously observed in systems involving interfacial instabilities.

In this Letter, we present experimental evidence which agrees quantitatively with the prediction that a parity-breaking bifurcation occurs in axisymmetric TVF. We report for the first time, to our knowledge, the experimental observation of propagating solitary waves in an axisymmetric Taylor-Couette flow. These solitary waves are spatially localized deformations of vortex pairs which propagate through a stationary background of Taylor vortices. They exist in the region of parameter space for which RP's model allows for localization of the parity-breaking mode. We also discuss some of the dynamics of the solitary waves and the protocol which we use to excite this localized mode. Our experiment verifies the existence of propagative parity-breaking dynamics in a noninterfacial pattern-forming system, which results from the resonant interaction of spatial modes.

The experiment was performed in a Taylor-Couette apparatus with an inner-to-outer-cylinder radius ratio of $\eta = a/b = 0.50$, which matches the value of η used in the theoretical analysis (outer-cylinder radius $b = 2.54$ cm). Delrin plastic end caps formed the end boundaries of the annulus. The position of one end cap was adjustable so that the length of the annulus could be varied. We varied the length L between 18.3 and 20.1 cm so that the length-to-gap aspect ratio $\Gamma = L/d$ ranged from 14.4 to 15.8 ($d = b - a$). The cylinders were driven by computer-controlled stepping motors with a resolution of 0.002 Hz or better. The fluid was 65% glycerin (by volume), 32% distilled water, 2% Kalliroscope rheoscopic agent for flow visualization, and 1% bacterial stabilizer [13]. For data acquisition, we used a frame grabber computer card and a 512 by 484 pixel charge-coupled-device (CCD) video camera. The frame grabber is capable of grabbing individual frames, or subsets of frames such as a row of pixels, for storage and analysis. We were able to record patterns in the fluid flow by storing video images of reflected light from the rheoscopic agent, which consists of highly reflective micron-sized platelets which respond to shear, thereby allowing patterns to be visualized. The inner- and outer-cylinder angular velocities ω_1 and ω_2 are scaled in terms of the inner-cylinder Reynolds number $R = a\omega_1 d/\nu$ and the speed ratio $\mu = \omega_2/\omega_1$, where ν is the kinematic viscosity of the fluid. To compare with theoretical calculations, our results are reported in terms of the reduced Reynolds number $\varepsilon = (R - R_c)/R_c$, where R_c is the critical Reynolds number for the onset of axisymmetric TVF.

In RP's linear stability analysis of axisymmetric TVF they found that for fixed outer cylinder, i.e., $\mu = 0$, the parity-breaking bifurcation exists for $\eta=0.5$, but it is preempted by an Eckhaus instability in which the stationary vortices become unstable with respect to long-wavelength perturbations. (This instability leads to a catastrophic creation of a vortex pair, i.e., a phase slip, so that the axial wave number q of the stationary pattern of vortex pairs is readjusted to lie within the Eckhaus stable band.) However, RP found that for a system with $\mu=-0.2$ (the negative sign indicates counterrotating cylinders) there is a range of wave numbers for which the parity-breaking bifurcation precedes the Eckhaus instability and should therefore be accessible experimentally. The parity-breaking mode which grows in at the onset of instability breaks the reflection symmetry of the vortex pairs and leads to (possibly localized) axial drift waves [8].

Using coupled nonlinear amplitude-phase equations to model the evolution of the parity-breaking mode, RP showed that there are stable solutions for the growth of the mode for which the wave number q is inhomogeneous. In parts of the system $q<q_{\mathrm{PB}}$, i.e., the static pattern is unstable, whereas in other parts $q>q_{\mathrm{PB}}$, where q_{PB} (which depends on ε) is the critical wave number for the onset of the parity-breaking bifurcation. The inhomogeneity in q can lead to an inclusion of drift waves, which is localized where $q<q_{\mathrm{PB}}$ and travels through the steady pattern with a group velocity which differs from the phase velocity of the waves [8]. Figure 1 is a diagram of the experimental protocol which we devised to excite a stable localized inclusion. The solid curve, which is based on RP's results in Ref. [10], indicates the Eckhaus stable band for axisymmetric TVF with $\eta=0.5$ and $\mu=0$. The dashed curve, which is based on RP's results in Ref. [8], is the bifurcation boundary with $\eta=0.5$ and $\mu=-0.2$. The lower end is the boundary for Eckhaus instability, the middle region is the boundary for the parity-breaking bifurcation, and the upper end is the boundary for a related Hopf bifurcation [8]. (There will be discussion below on the details of this bifurcation boundary.) As can be seen from the figure, counterrotation strongly deforms the bifurcation boundary, which is already somewhat deformed on the low-q side with the outer cylinder fixed. Both effects are due to resonant interaction of spatial modes with wave numbers q and $2q$ [8,10,12]. The neutral stability curves of the two modes cross, which creates an overlapping region above $\varepsilon\approx0.1$ where both modes are unstable, thereby deforming the bifurcation boundary. In step 1 of our protocol ε is increased quasistatically with the outer cylinder fixed, i.e., $\mu=0$, to a region near where the onset of the parity-breaking bifurcation would take place, if the cylinders were counterrotating with $\mu=-0.2$. In step 2 we adjust the end cap of the annulus so that locally the wave number of the vortex pair nearest the end cap would be less than q_{PB}, if $\mu=-0.2$. At this point the pattern is still stationary and the wave number for the vortex pairs throughout the system is inhomogeneous. The Ekman vortex at the very end of the annulus is also stretched by adjusting the end cap. In step 3, prior to diffusion of the change in wave number of the end vortex pair through the system, we rapidly spin-up the outer cylinder from a value of $\mu=0$ to $\mu=-0.2$. This last step causes the wave number of the vortex pair nearest the end cap to become unstable, while globally the wave number of the other vortex pairs in the system remains stable. We observe the onset of a localized, temporal disturbance of the unstable vortex pair which then drifts axially through the stationary pattern as a solitary wave.

Figure 2 is a position-time diagram in which successive time frames of a row of pixels, representing the intensity of light along the axial position z of the annulus, are plotted. The diagram shows a disturbance localized to one or two vortex pairs traveling through the otherwise undisturbed vortex pairs. This solitary wave reflects off the end caps of the annulus and travels back through the system. The stationary pattern shifts in the direction opposite to the direction of travel of the solitary wave, and shifts back to its original position when the wave travels back through the system. Sometimes the solitary wave

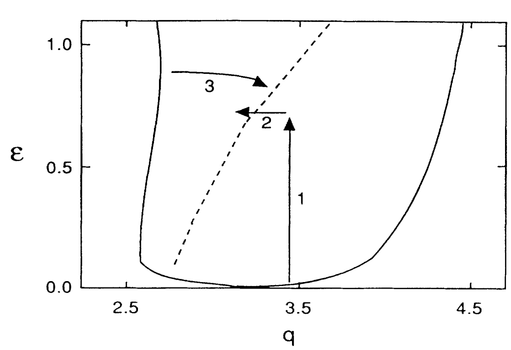

FIG. 1. Schematic diagram of the protocol used to excite stable solitary waves. See text for details.

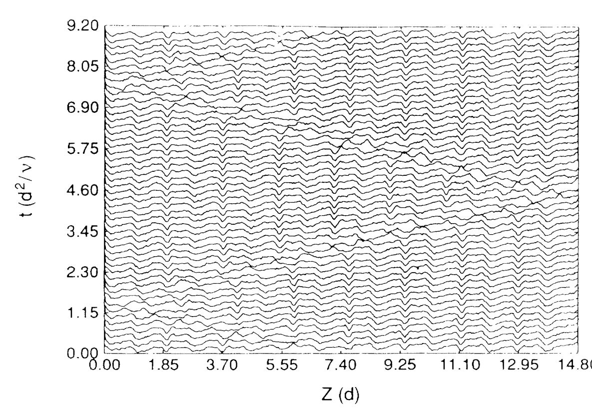

FIG. 2. Position-time plot of the solitary wave traveling through axisymmetric vortex pairs and reflecting off the end caps. The plot is for $\varepsilon=0.85$ and $q=3.47$, where q is the wave number for the undisturbed vortex pairs. The entire length of the system, with $\Gamma=14.8$, is shown.

acted as a long-lived transient eventually leading to a phase slip after approximately 100τ, where $\tau = d^2/\nu \cong 11$ s is the viscous diffusion time for our system. However, the solitary wave typically appeared to be a stable flow regime lasting more than 1000τ. In Fig. 3 we plot a single cycle of the solitary wave traveling from one vortex pair to the next. We smoothed the data with a smoothing function to eliminate high-wave-number noise due to small fluctuations in the rheoscopic agent [14]. Only part of the system, about four vortex pairs, is shown. Typically, the entire system contained seven vortex pairs and two Ekman vortices, one at each end cap. At $t=0$ s in Fig. 3 the solitary wave is primarily confined to one vortex pair, in the center of the plot, with the pair stretched asymmetrically. This is consistent with the disturbance resulting from a parity-breaking bifurcation which locally breaks reflection symmetry in a region in which $q < q_{\rm PB}$. At $t=1$ s the disturbance has stretched to encompass two vortex pairs. This is similar to stretching which precedes the creation of a new vortex pair in the Eckhaus instability. Instead, the solitary wave moves along to the next vortex pair as can be seen at $t=2.5$ s. The solitary waves we observed are remarkably similar to solitary waves which have been observed in an experiment on a moving nematic-isotropic liquid-crystal interface (compare Fig. 3 to Fig. 1 in Ref. [1]). The solitary waves in the directional solidification experiment also result from a parity-breaking bifurcation which occurs close to an Eckhaus instability [1,3–5]. There is also a striking similarity between the solitary waves which we excited and localized inclusions which form in a model, introduced by Coullet, Goldstein, and Gunaratne, for a parity-breaking bifurcation of a periodic pattern (compare Fig. 3 to Fig. 1 in Ref. [4]).

The solid and dashed curves in Fig. 4, which are calculated by RP from the basic equations of motion using linear stability analysis, are a more detailed version of the theoretical bifurcation boundary, for $\eta=0.5$ and $\mu=-0.2$, shown in Fig. 1 [15]. Below the dash-dotted line at $\varepsilon=0.3$, the solid curve is the bifurcation boundary for an Eckhaus instability. Above, it is the boundary for a parity-breaking bifurcation. The dashed curve is the boundary for a Hopf bifurcation. Above the dash-dotted line at $\varepsilon=0.84$, there is a critical crossing and the Hopf bifurcation should preempt the parity-breaking bifurcation. RP suggested that the Hopf bifurcation would lead to an "optical" oscillation mode involving adjacent vortex pairs in a standing-wave pattern [8]. In order to locate the parity-breaking and Hopf bifurcations experimentally, we adjusted the axial wave number q (with ε just above the onset of TVF) by adjusting the end cap of the annulus and allowing the wavelength of the vortex pairs to equilibrate throughout the system. Then ε was increased quasistatically while $\mu=-0.2$ was kept constant. The circles in Fig. 4 show where we found the onset of instability for TVF. Typically, at onset several solitary waves (the same in appearance as the single solitary wave in Figs. 2 and 3) would begin propagating through the system, often in opposite directions. This flow was transient. Within a short time (typically 10τ), usually when two disturbances collided, one or more new vortex pairs would be created and the entire system would return to a stationary state within the TVF stable region. This transient instability is consistent with the predictions of RP for the parity-breaking bifurcation. Their analysis showed that, exactly at onset, the parity-breaking bifurcation induces drift waves, which can propagate axially in either direction due to reflection symmetry prior to onset and are usually unstable with respect to sideband instabilities. This leads to a phase slip after a transient regime of drift waves, which takes the pattern back to an Eckhaus stable regime, as we observed experimentally. At no time did we observe the oscillation mode associated with the Hopf bifurcation [16]. However, RP's linear stability analysis did not allow any prediction as to the stability of

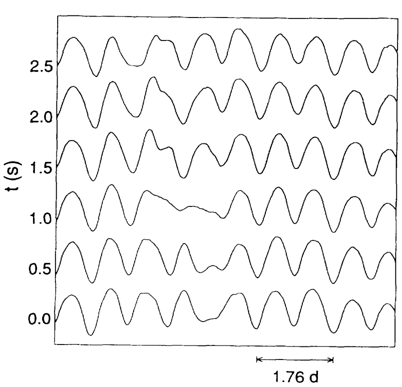

FIG. 3. Solitary wave propagating to the left with $\varepsilon=0.95$ and $q=3.57$. The sequence shows a single cycle of the solitary wave traveling between vortex pairs.

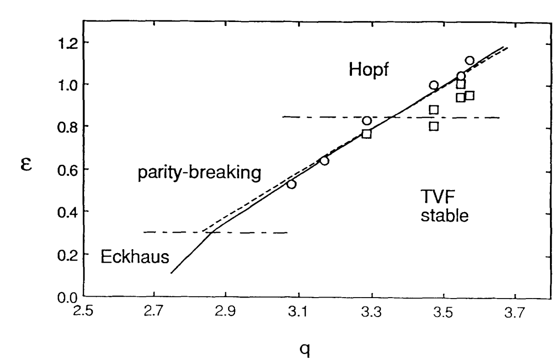

FIG. 4. Stability diagram for axisymmetric TVF. Circles indicate onset of transient flow leading to a phase slip. Squares indicate where stable solitary waves were excited. These latter data are plotted in terms of $q > q_{\rm PB}$, i.e., the wave number of the undisturbed vortex pairs. The dashed and solid curves are the theoretical boundaries for Hopf and parity-breaking bifurcations.

the oscillation mode. If the Hopf bifurcation is unstable at onset, it is not surprising that we observed the same transient instability in this region as we observed in the region for the parity-breaking bifurcation, since the theoretical bifurcation boundaries lie so close together. For example, RP found that at $\varepsilon = 1.02$ the Hopf bifurcation occurs at $q = 3.529$ and the parity-breaking bifurcation occurs at $q = 3.524$. The data represented by the circles are the first experimental measurements, to our knowledge, of these instabilities for axisymmetric TVF at $\eta = 0.5$ and $\mu = -0.2$ and show good quantitative agreement with the theoretical bifurcation lines.

The squares in Fig. 4 represent points in parameter space where we excited stable solitary waves. The data are plotted using the global wave number $q > q_{\mathrm{PB}}$ of the undisturbed vortex pairs, i.e., the wave number of the vortex pairs after step 2 in our protocol to excite a solitary wave. This wave number did not change for the undisturbed vortex pairs after a solitary wave was excited. We were unable to make an accurate measurement of the local wave number $q < q_{\mathrm{PB}}$ of a disturbed vortex pair, as it is difficult to determine the boundary of a solitary wave during the stretching of vortex pairs and traveling of the disturbance. As shown in Fig. 4, the globally stable wave number $q > q_{\mathrm{PB}}$ lies close to the theoretical line for the parity-breaking bifurcation, but in the TVF stable region as expected. Again it is not surprising that we observed behavior associated with the parity-breaking bifurcation in the region where it is slightly preceded by the Hopf bifurcation. It might be that the Hopf bifurcation leads to an unstable pattern (as mentioned above) or that creating an inhomogeneous wave number in the system breaks the symmetry necessary for a stable oscillation mode.

In conclusion, we have found strong experimental evidence that a parity-breaking bifurcation exists for TVF at $\eta = 0.5$ and $\mu = -0.2$, in agreement with the theoretical analysis of RP. The parity-breaking bifurcation can lead to a solitary wave which is either stable or a long-lived transient and travels axially through the stationary background pattern. The experiment verifies RP's conjecture that resonant interaction of spatial modes can generate a parity-breaking bifurcation leading to propagative dynamics in a noninterfacial pattern-forming system.

We would like to thank Professor Hermann Riecke and Professor Russell Donnelly for helpful discussions. In addition, we would like to thank Professor Donnelly for the use of some laboratory equipment. We would also like to acknowledge the late Don Nickles who modified the experimental apparatus to allow for counterrotation.

[a]Present address: College of Oceanography, Oregon State University, Corvallis, OR 97331-5503.

[b]Present address: Department of Physics, University of Oregon, Eugene, OR 97403.

[1] A. Simon, J. Bechhoefer, and A. Libchaber, Phys. Rev. Lett. **61**, 2574 (1988); J.-M. Flesselles, A. J. Simon, and A. Libchaber, Adv. Phys. **40**, 1 (1991).

[2] M. Rabaud, S. Michalland, and Y. Couder, Phys. Rev. Lett. **64**, 184 (1990).

[3] H. Levine, W.-J. Rappel, and H. Riecke, Phys. Rev. A **43**, 1122 (1990).

[4] P. Coullet, R. E. Goldstein, and G. H. Gunaratne, Phys. Rev. Lett. **63**, 1954 (1989).

[5] H. Levine and W.-J. Rappel, Phys. Rev. A **42**, 7475 (1990).

[6] W.-J. Rappel and H. Riecke, Phys. Rev. A **45**, 846 (1992).

[7] R. E. Goldstein, G. H. Gunaratne, L. Gil, and P. Coullet, Phys. Rev. A **43**, 6700 (1991).

[8] H. Riecke and H.-G. Paap, Phys. Rev. A **45**, 8605 (1992).

[9] A review of Taylor-Couette flow is given by R. C. DiPrima and H. L. Swinney, in *Hydrodynamic Instabilities and Transitions to Turbulence*, edited by H. L. Swinney and J. P. Gollub (Springer, Berlin, 1981).

[10] H. Riecke and H.-G. Paap, Phys. Rev. A **33**, 547 (1986).

[11] M. A. Dominguez-Lerma, D. S. Cannell, and G. Ahlers, Phys. Rev. A **34**, 4956 (1986).

[12] H.-G. Paap and H. Riecke, Phys. Rev. A **41**, 1943 (1990).

[13] For a discussion of the properties of Kalliroscope see P. Matisse and M. Gorman, Phys. Fluids **27**, 759 (1984).

[14] We used a routine which is analogous to the "smoothing of data" algorithm in W. H. Press, B. P. Flannery, S. A. Teukolsky, and W. T. Vetterling, *Numerical Recipes* (Cambridge Univ. Press, Cambridge, 1986).

[15] The dashed curve corresponds to a dimensionless Floquet parameter $p = \frac{1}{2}$, and the solid curve corresponds to p close to zero (see Ref. [8]).

[16] We attempted, without success, to excite the oscillation mode by temporally modulating the outer-cylinder angular velocity ω_2 in accordance with suggestions in Ref. [8]. This modulation affected TVF with a corresponding modulation in the amplitude of the vortices. The change in the steady-state pattern might be what made the modulation technique ineffective.